This article has been accepted for publication in a future issue of this journal, but has not been fully edited. Content may change prior to final publication. Citation information: DOI 10.1109/TNSRE.2021.3059015, IEEE Transactions on Neural Systems and Rehabilitation Engineering

A Soft Pressure Sensor Skin to Predict Contact Pressure Limit Under Hand Orthosis

Xinyang Tan[1], Saeema Ahmed-Kristensen[2], Jiangang Cao[3], Qian Zhu[3], Wei Chen[3], and Thrishantha Nanayakkara[1]

***Abstract*—Customized static orthoses in rehabilitation clinics often cause side effects, such as discomfort and skin damage due to excessive local contact pressure. Currently, clinicians adjust orthoses to reduce high contact pressure based on subjective feedback from patients. However, the adjustment is inefficient and prone to variability due to the unknown contact pressure distribution as well as differences in discomfort due to pressure across patients. This paper proposed a new method to predict a threshold of contact pressure (pressure limit) associated with moderate discomfort at each critical spot under hand orthoses. A new pressure sensor skin with 13 sensing units was configured from FEA results of pressure distribution simulated with hand geometry data of six healthy participants. It was used to measure contact pressure under two types of customized orthoses for 40 patients with bone fractures. Their subjective perception of discomfort was also measured using a 6 scores discomfort scale. Based on these data, five critical spots were identified that correspond to high discomfort scores (> 1) or high pressure magnitudes (> 0.024 MPa). An artificial neural network was trained to predict contact pressure at each critical spot with orthosis type, gender, height, weight, discomfort scores and pressure measurements as input variables. The neural networks show satisfactory prediction accuracy with R^2 values over 0.81 of regression between network outputs and measurements. This new method predicts a set of pressure limits at critical locations under the orthosis that the clinicians can use to make orthosis adjustment decisions.**

***Index Terms*—Wearable soft sensor, Contact pressure measurement, Discomfort, Orthosis.**

I. Introduction

IT is standard practice to customize static hand orthoses for patients in rehabilitation clinics. The customized orthosis stabilizes injured or diseased segments of the hand and wrist in a safe position, aiming to protect damaged tissues, facilitate recovery and delay muscular disorders [1]. Hand orthoses can have different forms to target various conditions. For example, the hand orthosis without thumb stabilization (WoTS) as shown in Fig. 1 is designated for conditions like distal ulna fracture. It immobilizes the wrist and the thumb carpo-metacarpal joint in the functional position without stretches. Fig. 1 shows another type of orthosis with thumb stabilization (WTS) in abduction, immobilizing the wrist in the same angle as WoTS, for conditions such as scaphoid fracture and first metacarpal base fracture. Poor patient adherence and reduced effectiveness of orthoses have been reported in clinics as contributing factors leading to more invasive surgical interventions [2]. As orthoses are required to be worn for a long period, discomfort and pressure sores [3] have become the main side effects due to excessive contact pressure.

To reduce excessive contact pressure, methods have been investigated by clinicians such as using soft material orthosis and adding paddings. However, a randomized controlled study showed that a lower level of orthosis effectiveness was found in the group wearing soft material splints than the group with rigid ones [4]. Soft paddings may result in skin blister or ulcers as it can cause constriction of skin areas with high contact pressure if the padding is wrinkled or not accurately placed at the critical location [5]. Another study [6] also showed that the paddings cannot significantly reduce deep tissue damage under pressure. Thus, alleviating patients' discomfort without decreasing orthosis effectiveness or changing the common splinting procedure in clinics remains a significant challenge.

Clinicians attempt to mitigate excessive contact pressure by adjusting the orthosis, relying upon the subjective feedback of patients [7]. The effectiveness of this approach is limited due to several reasons. Firstly, without clearly understanding the pressure distribution and magnitude, it is difficult to adjust at all critical locations and assess the adjustment accurately. Secondly, the sensation of discomfort may appear after patients have left the hospital, as the feeling of discomfort increases over time along with progressively aggravated tissue damage [8], thus preventing precise and real-time reports from patients. Thirdly, as ulcers usually occur at bony areas [9], contact at bony prominences may be noted by clinicians. However, excessive contact which is not close to a bony area is likely to

Fig. 1. The two types of hand orthoses and corresponding conditions.

This work was partly supported by the Affiliated Xuzhou Rehabilitation Hospital of Xuzhou Medical University, the Xuzhou Central Hospital, the China Scholarship Council and the Imperial College London. (Corresponding authors: Xinyang Tan, Wei Chen)

[1]X. Tan and T. Nanayakkara are with Dyson School of Design Engineering, Imperial College London, London SW7 2DB, UK xinyang.tan14@imperial.ac.uk

[2]S. Ahmed-Kristensen is with INDEX, Dept of Science, Innovation, Technology, Entrepreneurship, University of Exeter, London SE1 8ND, UK s.ahmed-kristensen@exeter.ac.uk

[3]J. Cao, Q. Zhu and W. Chen are with the Affiliated Xuzhou Rehabilitation Hospital of Xuzhou Medical University, Xuzhou City 221009, China chenwei2339@163.com

This article has been accepted for publication in a future issue of this journal, but has not been fully edited. Content may change prior to final publication. Citation information: DOI 10.1109/TNSRE.2021.3059015, IEEE Transactions on Neural Systems and Rehabilitation Engineering

be unnoticed. Finally, as individual patients have various sensitivity to pressure on the skin, the same contact pressure may lead to different discomfort levels, thus a standard adjustment may not fit all patients.

Therefore, this study aims to provide a quantitative measurement of contact pressure under static orthosis where excessive pressure at specific areas on the hand can be identified soon after or during the splinting process. It will improve efficiency of orthosis adjustment to minimize side effects and help reduce the need for subjective assessments by clinicians. Two tasks need to be accomplished to achieve this goal:

Task 1: Develop a generalized pressure sensor skin fitted to specific types of hand orthoses. Previous studies were conducted to measure contact pressure on human body. For example, Akiyama et. al. measured contact force on the thigh using pressure sensors embedded in the cuff of a lower-limb active orthosis to avoid skin injuries [10]. Hopkins et. al. integrated soft sensor strips into a lower limb prosthesis to measure comfort by providing socket pressure mapping during walking and standing [11]. In other studies [12] and [13], contact pressures were detected at the plantar surface using pressure sensor insoles for gait analysis of children with cerebral palsy. A pressure sensor mat was placed under a wrist orthosis for carpal tunnel syndrome to measure contact pressure with different wrist angles [14]. Moreover, contact pressure under a scoliosis orthosis was employed to regulate quality of fit using air pressure sensors in the study [15]. Although pressure values were obtained with various sensors, little effort has been invested into discovering a reasonable distribution of sensors which may lead to a more efficient data acquisition (i.e. only capturing necessary data) and fit to a larger population of patients in the clinic. Most studies used commercial sensors or placed sensor units evenly over contact area, which may not adapt to the complex geometry of the human body, especially for hands with multiple joints.

Our previous study [16] developed a soft sensor skin to measure contact pressure for a single subject wearing a hand orthosis. Sensor units of the skin were strategically distributed at high pressure spots extracted from finite element analysis (FEA). This enables us to develop a generalized sensor pattern to measure contact pressure from a large group of patients.

Task 2: Predict pressure limits at critical spots on the hand. To report excessive contact pressure, the pressure limit (i.e. a threshold of contact pressure that brings relatively high discomfort) at each key spot needs to be estimated, as the perception of discomfort varies at different locations on the skin. The correlation between perception of discomfort and contact pressure should be characterized. In the literature[17], comfort or discomfort was quantified as the maximum tolerable force loaded on the shoulder, thigh and shank, and it was reported to vary among participants. Regression statistics were applied in studies [18] and [19] to extract the correlation between comfort and contact force of gripping. In addition, an artificial neural network (ANN) was built in [20] to predict comfort level of automobile seat with contact pressure as one of the input variables.

However, most studies only reported the overall discomfort (comfort) rather than indicating the difference of discomfort (comfort) levels at specific locations within the large contact area. Also, little information was found regarding the discomfort-pressure correlation of static orthosis for real treatment in the rehabilitation clinic. Better understanding this knowledge gap enables us to predict pressure limit at critical spots. This will provide guidance for orthosis fabrication to conquer the side effects.

In the rest of this paper, methods of sensor pattern generation, patient data collection and building ANN for pressure prediction are demonstrated in section II. Results of data analyses and identification of critical spots are shown in section III. Further discussions and summary are presented in sections IV and V.

II. Methods

A three-step method was developed including: 1) sensor pattern generation, 2) data collection from patients, and 3) building an artificial neural network for pressure prediction. First, a FEA was conducted using 3D scanned hands and orthoses of six healthy subjects to simulate contact pressure distribution, i.e. identifying where an individual sensor pattern would fit on the hand of each subject. Then, a generalized sensor pattern was derived from the six distributions and this was used to fabricate the soft sensor skins. Second, the contact pressure under orthoses worn by 40 patients and their subjective feedback regarding discomfort were collected. These data were analyzed to identify critical spots potentially with excessive contact pressure. Finally, the patients' data were employed to train the neural network (NN) of individual key spot to predict the pressure limit. The data analysis and building of the NN were conducted in Matlab (R2018b, MathWorks USA).

A. Sensor pattern generation

1) Generating individual sensor patterns: Six healthy subjects (three male and three female) were recruited and their informed consent was received. A hand orthosis with thumb stabilization (WTS) was custom-fabricated for each of them by experienced senior clinicians. Each of the three male/female subjects had low, middle and high body mass index (BMI) respectively according to [21]. A six-step process was conducted to extract individual pressure distribution as shown in Fig. 2a.

- The hand of a subject wearing the orthosis was 3D scanned. The physical reference for positioning (PRP) and the physical references for assembly (PRA) were designed in a CAD software and 3D printed.
- The PRP (yellow) was temporarily attached on the hand to modify the joints into the correct angles as if wearing the orthosis and the subject was asked to keep the hand steady in this position. The PRA (red) and PRA (blue) were attached on the orthosis and hand respectively. The hand and the orthosis with PRAs were 3D scanned and the PRAs were used to assist assembly of the hand and orthosis models in the CAD software by simply matching the blue and red PRAs together.
- The hand and orthosis models were assembled and processed in the CAD software to remove extra parts.

This article has been accepted for publication in a future issue of this journal, but has not been fully edited. Content may change prior to final publication. Citation information: DOI 10.1109/TNSRE.2021.3059015, IEEE Transactions on Neural Systems and Rehabilitation Engineering

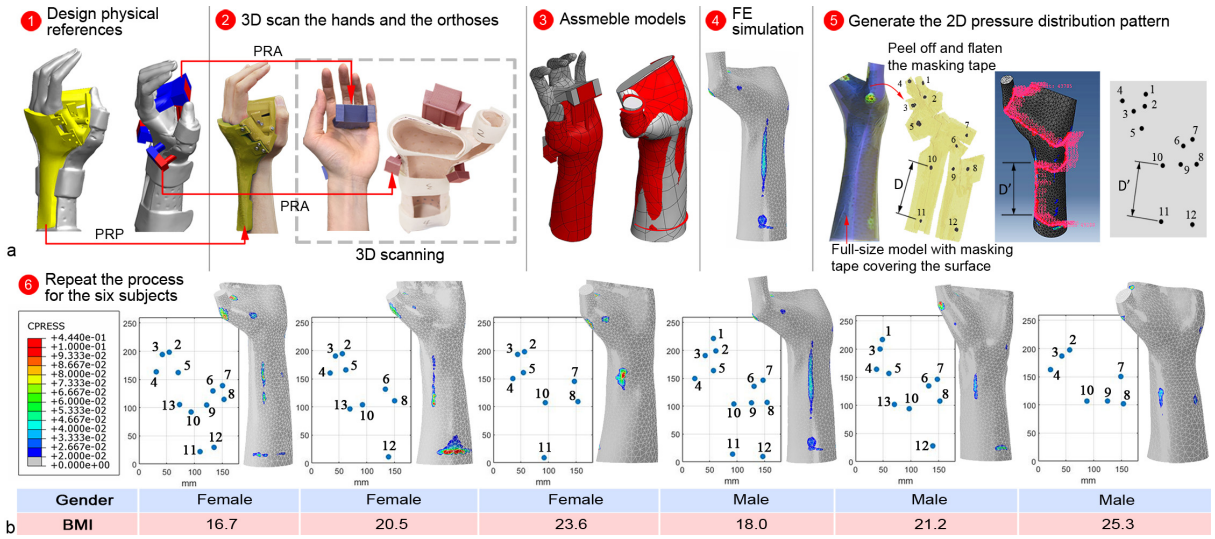

Fig. 2. a. The process of generating individual pressure distributions. At step 1 and 2, the PRP was used to hold the hand in the functional position. The blue and red PRAs were attached to the hand and orthosis respectively to assist model assembly in CAD. At step 5, the pressure distribution of the FEA result was projected on a 3D printed hand model and pressure spots were marked manually on the masking tape. A rough pressure distribution was obtained by peeling off and flattening the masking tape. Distances between any two spots (e.g. D) was measured. Then, the accurate distance (e.g. D') was obtained in Abaqus using the path function. Thus, distances could be corrected (change D to D') to achieve an accurate pressure distribution. b. Individual pressure distributions of the six subjects and their corresponding BMI.

Compared with our previous study [16], the hand bones were not included in the assembly models of the six subjects. As the contact pressure is generated due to the interference fit of the hand and orthosis, the bones embedded inside the hand mainly affect the pressure magnitude with little influence on the pressure distribution. Since the focus of this procedure is to gain the pressure distribution, there is no necessity to include bones in the model.

- The FEA was conducted in Abaqus (Abaqus 2018, Dassault Systemes, France) with the skin material parameter (Young's modulus = 0.177 MPa, Poisson's ratio = 0.45) assigned to the hand model and the orthosis material parameter (Young's modulus = 393.3 MPa, Poisson's ratio = 0.34) set for the orthosis shell. The FEA results of the six subjects are shown in Fig.2b.
- The pressure spots scattered over the 3D hand model were converted into a 2D pressure distribution pattern (see Fig.2a-5).
- The process was repeated to attain the six individual sensor patterns. All pressure spots found in simulation results were distributed in 13 anatomical locations as showed in Fig. 2b.

2) Creating the generalized sensor pattern: To obtain a generalized sensor pattern fitting to a larger group of subjects, the six individual sensor patterns were imported into a single coordinate. The 13 spots were divided into three groups (see Fig. 3a), since spots in different groups were relatively far from each other on the hand and it was easier to generate the one-for-all pattern if spots nearby can be grouped together. Then two steps were followed to concentrate spots of different subjects in the same group: (1) selecting any individual sensor pattern as the base pattern; (2) moving the spots in a group of any other individual pattern and aligning them to the corresponding spots in the same group of the base pattern

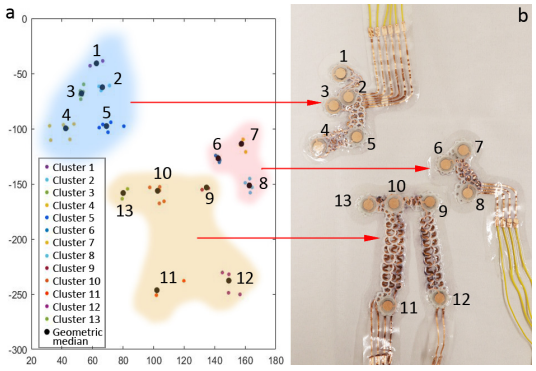

Fig. 3. a. 13 spots were divided into three groups with the first group near the thumb, the second one near the distal ulna and the last one near the palm side of the forearm and the distal radius. b. The generalized sensor pattern with three separated skin pieces.

without changing the relative position of included spots. It was completed through calculating and optimizing the sum of distances between each pair of corresponding spots in the base and the selected group until the minimum value was obtained. Hence, all individual sensor patterns were split into three groups and spots of different subjects within the same group were concentrated. Afterwards, the k-means clustering was performed to partition the data into 13 clusters using the Lloyd's algorithm [22]. The aim of the clustering is to verify that the pressure spots at the same anatomical location from different simulations were placed as close as possible so that they can be reached by the sensor unit of the generalized sensor pattern without over-stretching the sensor skin. It took 200 replications for the algorithm to find the minimum sum of point-to-centroid distances (337.31 mm) of the 13 clusters. The result shows that all spots at the same anatomical location were grouped in the same cluster, validating a reliable grouping.

This article has been accepted for publication in a future issue of this journal, but has not been fully edited. Content may change prior to final publication. Citation information: DOI 10.1109/TNSRE.2021.3059015, IEEE Transactions on Neural Systems and Rehabilitation Engineering

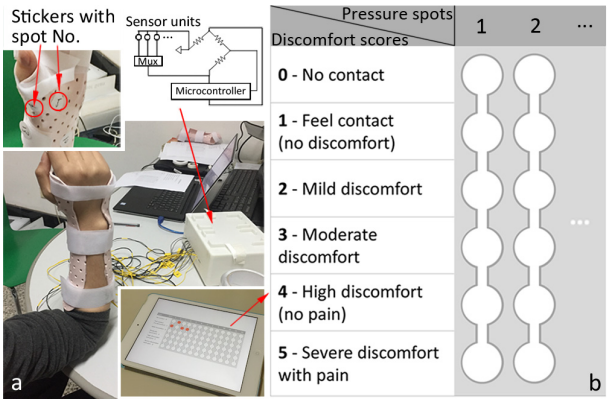

Fig. 4. a. Setup of patient testing. All sensor units were connected to a Wheatstone bridge through a multiplexer and data was collected using a microcontroller. b. Subjects were asked to select scores (0 to 5) at each pressure spot according to their subjective feeling of discomfort using the discomfort scale.

Finally, the geometric median of spots in each cluster was calculated using the Weiszfeld's algorithm which generated a point with minimum sum of absolute distances to all spots in a cluster. These points formed the one-for-all sensor pattern which was used to fabricate the three pieces of pressure sensor skins as shown in Fig. 3b. Although, there are still distances between the spot of an individual sensor pattern and the corresponding spot of the generalized pattern, due to flexibility of the sensor skin, each spot was able to reach its anatomical location on hands of all subjects during the data collection.

B. Data collection from patients

1) Subjects: Data was collected from 40 patients (19 male and 21 female). They were prescribed one of the two types of hand orthoses (22 WTS and 18 WoTS) by doctors depending on their conditions. Data regarding their orthosis type, gender, standing height and weight was collected, as well as their subjective perception of discomfort and objective measurement of contact pressure. Orthoses were custom-fabricated for each patient using a 3 mm thickness low temperature thermoplastic material (Klarity Medical Ltd., China) by experienced senior clinicians from the Rehabilitation Department at the Xuzhou Central Hospital. Consents from patient participants and clinicians were obtained. Patients must be over 18 years old and able to provide independent consent to join in the study. Five exclusion criteria were considered during the recruitment: (1) Patients with diabetes, paresthesia or sensation loss on hands; (2) Patients with open wounds on the hand, the wrist or the forearm of the affected side; (3) Patients with skin conditions, including blister, ulcer, rash, burn and other skin diseases on the hand, the wrist or the forearm of the affected side; (4) Patients with adhesive allergies; (5) Patients in whole day care or with mental illness or cognitive symptoms. Eligible patients were selected by clinicians and the researcher introduced the study when they came to the clinical room to have their orthoses customized. All participants joined the study voluntarily and they could withdraw at any time. Patients data was kept anonymously and confidentially. The protocol has been approved by the Xuzhou Central Hospital

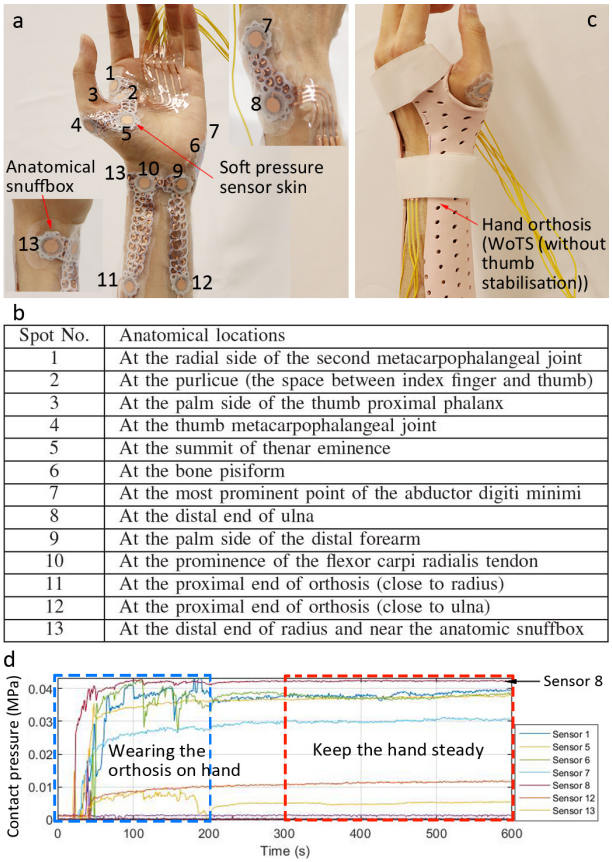

Spot No.	Anatomical locations
1	At the radial side of the second metacarpophalangeal joint
2	At the purlicue (the space between index finger and thumb)
3	At the palm side of the thumb proximal phalanx
4	At the thumb metacarpophalangeal joint
5	At the summit of thenar eminence
6	At the bone pisiform
7	At the most prominent point of the abductor digiti minimi
8	At the distal end of ulna
9	At the palm side of the distal forearm
10	At the prominence of the flexor carpi radialis tendon
11	At the proximal end of orthosis (close to radius)
12	At the proximal end of orthosis (close to ulna)
13	At the distal end of radius and near the anatomic snuffbox

Fig. 5. a. Soft sensor skins attached on the hand; b. Anatomical locations of pressure spots; c. Hand orthosis worn on top of the sensor skin; d. Signal of contact pressure collected from the sensor skin.

Biomedical Research Ethics Committee (XZXY-LJ-20190222-003, 22/02/2019) and the Imperial College Research Ethics Committee (19IC5128, 26/04/2019).

2) Contact pressure measurement: After going through the normal customization process by the clinician, including adjustments as needed based on feedback from the patient, the subject was asked to raise up the affected hand and put the elbow on the table (see Fig. 4). The three pieces of soft sensor skins (thermoplastic polyurethane-based, 0.8mm thickness) were attached on the hand using silicone tapes (see Fig. 5a). Each sensor unit was placed at the corresponding anatomical location as shown in Fig. 5b with assistance from the clinicians. Care was taken not to press hard when attaching the sensors and the hand of the subject should be supported gently by a clinician. Then, the completed hand orthosis was worn properly on top of the soft sensor skins (see Fig. 5c). It was essential to guarantee that there was no wrinkle or fold of the sensor skin that may cause discomfort. The straps of the orthosis should be fastened as predefined by the clinician with appropriate tightness. All subjects reported that there was no notable difference between with and without the sensor skins when wearing the orthosis. Then, the subject was asked to hold the hand steady for about 15 minutes. Since slight motion of the hand was inevitable, the relatively stable data of 5 minutes was selected from the raw data (see Fig. 5d) and the mean was calculated for further analysis. After 10 minutes, the subject

This article has been accepted for publication in a future issue of this journal, but has not been fully edited. Content may change prior to final publication. Citation information: DOI 10.1109/TNSRE.2021.3059015, IEEE Transactions on Neural Systems and Rehabilitation Engineering

started reporting the subjective perception of discomfort. As patients were not able to see the real-time values of contact pressure, their subjective judgments were not affected by the measurement.

3) Collection of subjective perception of discomfort: Stickers with the spot No. were adhered on the orthosis at anatomical locations. A categorical discomfort scale [23] was used to measure subjective perception of patients. As shown in Fig. 4b, the discomfort is represented by six categories with "no contact" assigned with the score zero and "severe discomfort with pain" labeled at the score five. These two scores at the ends of the scale line are more explicit than other scores, as it should be easy for patients to subjectively decide if there is a contact or pressure pain at the spot, leaving less room for confusion, thus setting up a fixed range of measurement and freeing from bias of feeling of different subjects. Moreover, scores in columns of all spots were presented in a single form, so the subject could refer to previous selections when making decisions. An introduction was provided to all subjects to ensure full understanding of the scale. During the subjective measurement, the researcher pointed at each pressure spot on the hand of the subject without actually touching the hand, and the subject was asked to select the discomfort score according to their subjective perception at that spot. Enough time should be allowed for subjects to feel the discomfort of contact and distinguish it from other interruptions, such as discomfort at other locations or pain of the condition. The process was conducted twice, thus subjects could compare any score relatively among others to minimize errors. Subjects could change scores at any time during the procedure which took about five minutes. Afterwards, the sensor skins were removed from the hand and the data collection completed. A concern was raised that the pain of injuries would disturb the judgment of patients regarding discomfort, as pain is commonly reported in fracture due to soft tissue damage and friction of broken bone pieces. However, the pain was largely reduced when wearing the orthosis as it immobilized the limb and prevented the friction. The orthosis also supported muscles near the injury so the patient did not need to hold it using their own strength. Thus, the subjective measurement was not severely affected by the pain.

Data collected from the 40 subjects were analyzed from several aspects to identify critical spots: (1) Principal component analysis (PCA) was performed to justify if the type of orthosis was a notable factor; (2) The pressure data and the discomfort scores were compared among spots and between the two types of orthoses. The Shapiro-Wilk test showed these data at each spot were nonparametric ($p < 0.05$); (3) The ratios of discomfort score to contact pressure were calculated and; (4) Five critical spots with excessive contact pressures were identified. Detailed results of the analyses were reported in section III.

C. Building artificial neural networks for pressure prediction

Five feed-forward fully-connected ANN were built for the five critical spots. Each ANN was constructed with a sigmoid hidden layer and a linear output layer. The ANN models were trained with the Levenberg-Marquardt back-propagation algorithm using data from all subjects, including orthosis type, gender, standing height (m), weight (kg) and discomfort scores as the input data. The contact pressure at each spot was used as the target data. Specifically, 0 and 1 were assigned to WTS and WoTS respectively as the variable of orthosis type, and 0 and 1 were also referred to female and male in the gender variable. The height and weight were included in the data, as the hand geometry is related to the body shape [24]. The input data were divided into training set, validation set and testing set with a ratio of $70\% : 15\% : 15\%$. The training set was used for training the NN, updating weights and biases, while the validation set was used to validate the generalization of the network and to terminate the training before the model was overfitted. The testing set was used independently for testing the ANN performance. The training of each NN was conducted several times with initialized training parameters and shuffled samplings of the three sets to maximize R^2 values of the training set and the testing set. Different architectures were tested with different proportions of sample sets and number of hidden neurons to achieve relatively low mean squared error (MSE). The number of hidden neurons was increased one by one until a satisfactory accuracy was achieved without overfitting. Some hyper-parameters of the five ANN models can be seen in Table I. The fitting between the ANN outputs and the target testing data presents high R^2 values (i.e. high proportion of the data variation explained by the linear model), indicating satisfactory linear relationship between the measurements and network outputs, thus all the five ANN models show satisfactory regression prediction accuracy.

TABLE I
NEURAL NETWORK HYPER-PARAMETERS AND PERFORMANCE EVALUATION

Spot No.	3	4	7	8	13
Hidden neuron amt.	4	4	5	12	5
Training sample size	28	28	28	28	28
Validation sample size	6	6	6	6	6
Testing sample size	6	6	6	6	6
R^2 (training)	0.88	0.91	0.81	0.81	0.86
R^2 (testing)	0.90	0.97	0.88	0.81	0.89
MSE (testing)	1.25e-5	1.71e-5	3.86e-6	6.14e-6	4.47e-6

III. RESULTS

A. Contact pressures and discomfort scores of all subjects

The contact pressures and discomfort scores at all spots of the 40 subjects were reported in Fig. 6 and a Pearson's

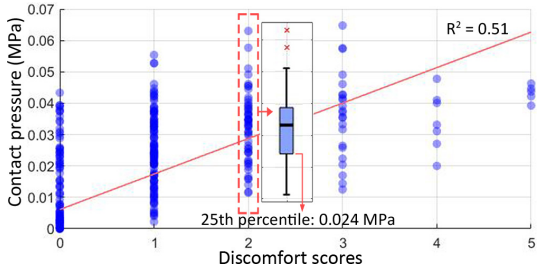

Fig. 6. Contact pressures and discomfort scores at all spots of all subjects.

This article has been accepted for publication in a future issue of this journal, but has not been fully edited. Content may change prior to final publication. Citation information: DOI 10.1109/TNSRE.2021.3059015, IEEE Transactions on Neural Systems and Rehabilitation Engineering

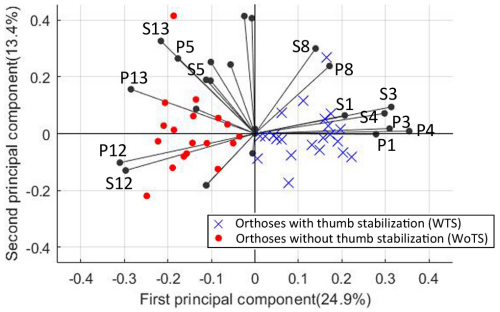

Fig. 7. Results of principal component analysis. P and S refer to the variables of contact pressure and discomfort score respectively. The number following P or S indicates the spot No.

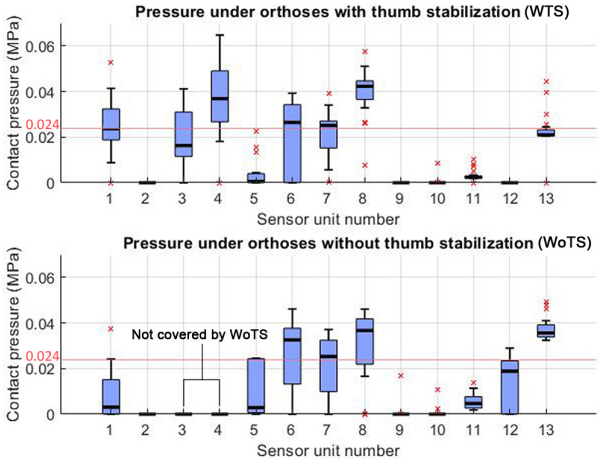

Fig. 8. Box plots of contact pressure at each pressure spot under the two types of orthoses

r test was conducted to investigate if they were correlated, regardless of the location of contact. The result showed a positive correlation ($p < 0.01$) with low linearity ($R^2 = 0.51$). Eight subjects reported discomfort with high or severe level (score 4 and 5) at one or two spots. To initially define a threshold of contact pressure which may bring discomfort, the 25th percentile of contact pressure at the discomfort score 2 (mild discomfort) was calculated as 0.024 MPa. The 25th percentile can provide a meaningful benchmark of contact pressure to distinguish 75% of patients who reported mild level of discomfort. Statistically, the 25th percentile is the low limit of the interquartile range (25% to 75%) which represents most data and it has been widely employed in clinical studies as a threshold. For example, the study [25] applied the 25th percentile to define a safe range of wrist angles for patients with carpal tunnel syndrome. The threshold was used in the section III-C to identify spots with high pressure magnitudes.

In addition, it can be noted that non-zero contact pressure was measured at the discomfort score 0 ("no contact"). Since the discomfort scores were reported based upon the subjective perception, it was expected that subjects felt no contact, but in fact contact existed. This may be due to two reasons: (1) The subjective perception of local contact was interfered when a large skin area was covered. (2) Some areas that were reported "no contact" have low contact sensitivity. Thus, the contact was overlooked or could not be perceived by participants.

B. Principal component analysis (PCA)

The PCA was conducted to initially investigate if the orthosis type affected the objective and subjective measurements at each spot with 26 variables including the contact pressure and discomfort scores of all subjects at the 13 spots. All data were normalized by computing the z-score with 0 as the center and standard deviation (SD) of 1. The normalization ensured that all variables were treated equally in terms of scale. The PCA was performed using the singular value decomposition algorithm. The principal component scores were highlighted regarding the two types of orthoses, i.e. WTS and WoTS, in the PCA result reported in Fig. 7. It can be seen from the result that subjects wearing WTS (blue) are distinct from subjects wearing WoTS (red) in terms of the first principal component. Variables related to sensors 1, 3, 4, 5, 8, 12 and 13 have relatively greater impact on the first principal component than other variables. Specifically, subjects with positive scores at the first principal component have greater values of P1, P3, P4 and P8, as well as their corresponding variables of discomfort scores, indicating patients with WTS may report higher contact pressure and discomfort at these locations. It was expected to have higher values at spots 3 and 4 as the two locations were covered only under WTS. Moreover, spots 5, 12 and 13 show relatively lower negative principal component scores at the first component. Hence, higher pressures and discomfort scores may be measured from subjects wearing WoTS at the three spots. Most importantly, the PCA revealed different situations of wearing the two types of orthoses. Thus, the orthosis type should be taken into consideration when analyzing measured data.

C. Pressure magnitude at each spot

The box plots of contact pressures at each spot of subjects wearing WTS and WoTS were shown in Fig. 8. Spots with median value over the pre-defined threshold (0.024 MPa) were considered as ones with high pressure magnitudes, including spots 4, 6, 7 and 8 for subjects wearing WTS, and spots 6, 7, 8 and 13 for subjects wearing WoTS. Low or no contact pressure was measured at 4 out of 13 spots (No. 2, 9, 10 and 11), possibly because they were located at very soft tissues on the hand. For instance, sensor unit 2 was placed on top of the purlicue, where almost no pressure was detected. Moreover, it was expected that no pressure data was gained at spots 3 and 4 from subjects wearing WoTS as the areas were not covered by orthoses.

The Mann-Whitney U test was performed to understand if contact pressures at the same spot were different between the two types of orthoses and validate the results from PCA. The results showed that contact pressures at spots 1 (mean = 0.023 MPa) and 8 (mean = 0.04 MPa) of WTS were significantly higher than contact pressures at the same locations of WoTS with average values of 0.008 MPa and 0.031 MPa respectively ($p < 0.05$), whereas pressure values at spots 5 (mean = 0.004 MPA), 12 (mean = 0 MPa) and 13 (mean = 0.021 MPa) of WTS were lower than WoTS with mean values of 0.011 MPa (

This article has been accepted for publication in a future issue of this journal, but has not been fully edited. Content may change prior to final publication. Citation information: DOI 10.1109/TNSRE.2021.3059015, IEEE Transactions on Neural Systems and Rehabilitation Engineering

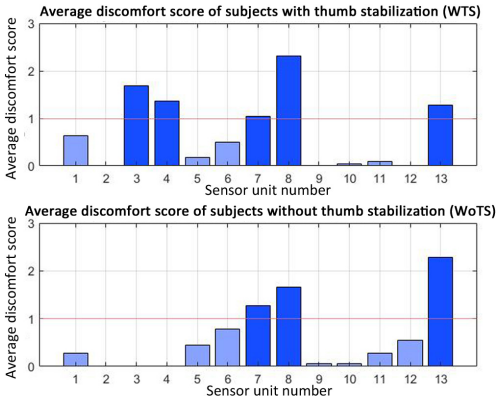

Fig. 9. Average discomfort score at each pressure spot

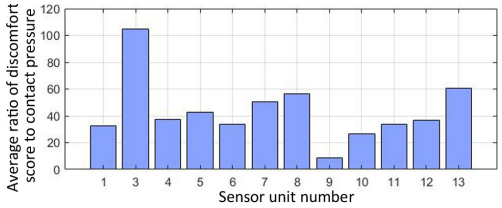

Fig. 10. Ratio of discomfort score to contact pressure at each pressure spot. As there was no contact pressure detected at spot 2 from all subjects, its ratio was not calculated.

$p = 0.012$), 0.015 MPa ($p < 0.01$) and 0.038 MPa ($p < 0.01$) respectively. The results of Mann-Whitney U test conformed to the trend shown in results of PCA.

D. Discomfort score at each spot

The average discomfort scores at each spot of subjects wearing WTS and WoTS are shown in Fig. 9. The discomfort score 1 ("contact but no discomfort") was set as the threshold. Thus, discomfort may be perceived at spots with average scores higher than the threshold. For subjects wearing WTS, high discomfort scores appeared at spots 3, 4, 7, 8 and 13. Pressure spots 7, 8 and 13 were also reported with high average scores by subjects wearing WoTS. The Mann-Whitney U test was conducted to compare whether there were differences of discomfort scores (excluding spots 2, 3 and 4) between the two types of orthoses. The result indicated that higher discomfort scores were found at spot 1 ($p < 0.05$) reported by subjects wearing WTS than those wearing WoTS, and they both showed relatively low values. Also, greater discomfort scores were reported at spots 5 ($p < 0.05$), 12 ($p < 0.01$) and 13 ($p < 0.01$) under WoTS than WTS. The results complied with the differences of pressure magnitudes at the four locations (spots 1, 5, 12 and 13). No significant difference was found at spot 8, maybe due to small sample size.

E. Ratio of discomfort score to pressure

Although from the previous analysis, a positive correlation was derived between subjective and objective measurements of all subjects, the sensitivity of contact pressure at different locations on the hand can vary. To generally compare the sensitivity among the spots, the average ratios of discomfort score to contact pressure at individual spot are reported in Fig. 10. Though the ratio cannot biologically represent the sensitivity of the hand, with the same contact pressure, higher discomfort score generally indicates that the spot responds to contact pressure more easily. Relatively higher ratios were found at spots 5, 7, 8, 13 and the spot 3 was revealed with the highest value.

F. Identify critical spots with excessive pressure

As the purpose of this study is to reduce discomfort due to excessive contact pressure under the two types of orthoses, the critical spots were determined, taking the high discomfort score (mean value > 1) and high contact pressure (median value > 0.024 MPa) into consideration. Five critical spots were identified based on the results, with spots 7, 8 and 13 for subjects wearing WoTS and two additional spots 3 and 4 for subjects wearing WTS. Specifically, spots 7 and 8 both showed high measurements of contact pressure and discomfort scores. Five (12.5%) and ten (25%) of 40 subjects reported moderate or greater discomfort (scores ≥ 3) at spot 7 and 8 respectively. At the spot 3 and 13, moderate contact pressures were detected, but the average discomfort scores were high as 1.7 and 1.3 respectively. Also, moderate or greater discomfort was felt by 27.3% and 17.5% subjects at the two locations. Hence, the spot 3 and 13 were selected as critical spots with excessive pressure. Moreover, high contact pressures and discomfort scores were reported at the spot 4 and four out of 22 subjects (18.2%) reported moderate discomfort, so excessive pressure may also occur at this location. Although relatively high pressure was found at spot 6, very low average discomfort score was reported and only one subject described discomfort over mild level. Thus, spot 6 was not considered as a critical spot.

To predict the pressure limits at the identified critical spots, the contact pressures and discomfort scores at each spot were plotted in Fig. 11. Only data from subjects wearing WTS were plotted for spot 3 and 4. Only moderate and higher discomfort (score ≥ 3) is essential to be mitigated, as completely avoiding discomfort is impossible when wearing rigid static orthoses which immobilize the hand in a fixed position. Thus, mild discomfort (score = 2) should be acceptable. The results of Pearson's r tests showed that the positive correlation between contact pressure and discomfort score was found at all critical spots ($p < 0.05$) with low correlation coefficients (range from 0.46 to 0.66). Therefore, data were used to fit to multi-degree polynomials from quadratic to quantic using the Least-squares fitting method. The highest R^2 values were 0.36 (degree 4), 0.27 (degree 3), 0.41 (degree 5), 0.58 (degree 5) and 0.58 (degree 5) at the spot 3, 4, 7, 8 and 13 respectively, indicating low fitting of the data to the polynomial models, likely due to the large variance of contact pressure at each discomfort score. Thus, this method could not provide a strong fitting of contact pressure and discomfort measurements for predicting the pressure limit.

G. Pressure limit prediction using neural network

The established NN was applied to predict the pressure limit at each critical spot that can result in moderate to

This article has been accepted for publication in a future issue of this journal, but has not been fully edited. Content may change prior to final publication. Citation information: DOI 10.1109/TNSRE.2021.3059015, IEEE Transactions on Neural Systems and Rehabilitation Engineering

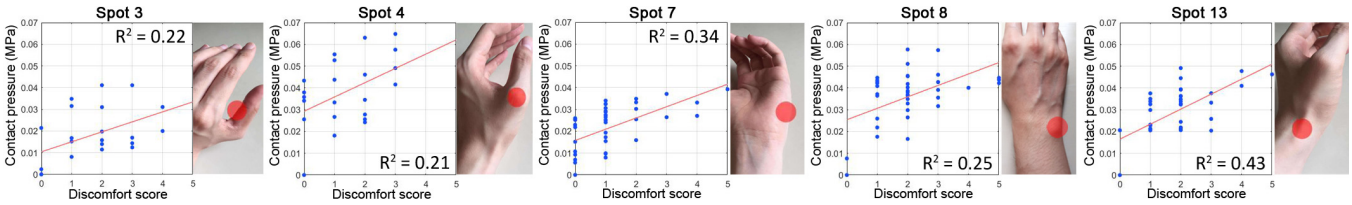

Fig. 11. Correlation between contact pressures and discomfort scores at each identified critical spot.

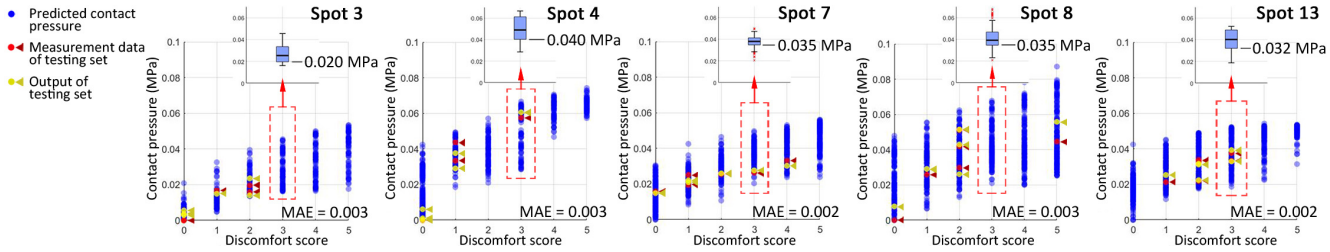

Fig. 12. Prediction of contact pressures (blue) at each critical spot using neural networks with 1000 randomly generated data. The measurement data (red) and output data (yellow) of testing set were also plotted. The mean absolute error (MAE) between measurement and output of testing set was reported.

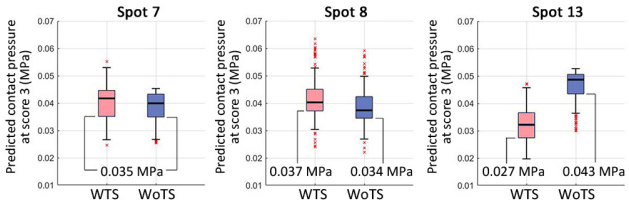

Fig. 13. Box plots of predicted contact pressures at discomfort score 3 for spots 7, 8 and 13 under each type of orthosis.

severe discomfort. One thousand data were generated as the input with the five variables. The orthosis type was randomly produced with values 0 or 1 as well as the variable of gender. Normally distributed data of height were randomly generated using the anthropometry data of local population with the mean of 1.66 m (SD = 0.066) for male and the mean of 1.56 m (SD = 0.059) for female. Also, the data of weight were randomly extracted from a normal distribution with the mean of 64.3 kg for male and 56.2 kg for female with SD of 10.3 and 9.1 respectively. Finally, random integers from 0 to 5 were input as the fifth variable to represent discomfort. For networks of spots 3 and 4, if the randomly generated orthosis type was WoTS, the input data of discomfort score was 0 as there should be no contact. The outputs of the five NN were reported in Fig. 12 with the box plot of contact pressures at score 3, and the pressure limit at each spot was defined as the 25th percentile as shown in the figure. Most data over this threshold may cause moderate or higher discomfort. The lowest pressure limit was at the spot 3 (0.02 MPa), which implied the highest sensitivity to contact pressure among all critical spots. This result conformed to the highest ratio between discomfort score and contact pressure at this location reported in section III-E. The highest pressure limit was found at the spot 4 (0.04 MPa), corresponding to the lowest ratio of discomfort to pressure. Thus, the predicted general pressure limits complied with the ratio calculations in terms of sensitivity at the five critical spots. In addition, contact pressures only for WTS or WoTS were also predicted with one thousand randomly generated data. The result showed that, at spot 3 and 4, contact pressure of all predictions for WoTS was close to 0 MPa. As shown in Fig. 13, the pressure limits at spot 7 for WTS and WoTS were the same as 0.035 MPa. The pressure limit at spot 8 for WTS was a bit higher than WoTS, whereas the pressure limit for WoTS was higher than WTS at spot 13.

IV. Discussion

A. Different pressures between the two types of orthoses

The higher pressure at spot 1 of WTS than WoTS may be explained that, when making the orthosis with thumb stabilization, the material was molded on the hand to fit to the purlicue, thus adding more pressure at the radial side of metacarpophalangeal joint of the index finger. The magnitudes at spots 5 and 13 were greater when the thumb was not stabilized, since the orthosis was fitted around the abductor pollicis brevis and firmly in contact with the two spots. Moreover, the pressures measured at spot 8 under WoTS were lower than WTS. It was possibly because clinicians took more care to adjust the orthosis near the injury (distal ulna fracture) to reduce the nearby pressure. But since injuries of WTS mostly occurred at the radial side, spot 8 was not the prime area to be adjusted. Thus, pressure could accumulate at this bony prominence under WTS.

B. Different pressure limits at the same spot

From the above results, the pressure limits at the same spot could be different between WTS and WoTS. This indicated that patients wearing different types of orthoses may have different sensitivity to pressure at the same critical spot. For example, subjects wearing WoTS with distal ulna fracture were a bit more sensitive to pressure at spot 8 which was close to the injury. Subjects wearing WTS with conditions at the scaphoid bone paid more attention to contact locally at the spot 13 than subjects with other wrist conditions. Though subjects

This article has been accepted for publication in a future issue of this journal, but has not been fully edited. Content may change prior to final publication. Citation information: DOI 10.1109/TNSRE.2021.3059015, IEEE Transactions on Neural Systems and Rehabilitation Engineering

were advised to distinguish between the discomfort caused by contact pressure and the pain of the condition, it was inevitable that the subjective perception at the two critical spots (8 and 13) was influenced by the nearby injuries. As spot 7 was not close to any affected area, the pressure limit was similar under both types of orthoses. Therefore, the pressure limit may vary according to the orthosis type. As part of our future study, the correlation between specific conditions and pressure limits will be investigated to further clarify the results and the variable related to conditions will be involved in the NN.

C. Critical spots not located at bony area

The occurrence of discomfort and pressure sores was conventionally considered at bony prominences [9]. However, two of the five critical spots, i.e. spots 3 and 7, are not located at bony areas. This indicates that soft tissues may also show high sensitivity to pressure. This can be explained anatomically that the pacinian corpuscles concentrate in skin at proximal phalangeal regions and hypothenar which are close to the two spots [26]. By contrast, a bony prominence may not bring high discomfort. For example at the bone pisiform (spot 6), low average discomfort score was reported. Therefore, the two spots 3 and 7 that are not located near bones and easily neglected by clinicians during customization were disclosed.

D. Reasons of recruiting healthy and patient subjects

The geometrical data was collected from healthy subjects to derive the generalized sensor pattern rather than directly 3D scanning patients' hands. First, it is difficult to obtain geometrical data from patients as the injuries prevent them from holding the hand stably in a pre-defined position without external support during 3D scanning. Second, though there were slight geometrical differences between healthy and injured hands, e.g. swelling near fractured bones, the difference was not significant for application of sensors due to flexibility of the sensor skins. However, if this method is applied to extract a sensor pattern for orthoses treating large-scale disorders, e.g. scoliosis, the geometrical data can be directly collected from patients if the body segment can be easily scanned without complex positioning. In addition, though the sensor pattern was generated based on data of healthy subjects, the pressure limits were predicted using patients data, since patients may have different perceptions from healthy people. Therefore, considering the clinical practice, small amount of geometrical data was collected from healthy subjects and a patient study was conducted to reveal the real situation of wearing orthoses.

E. Difference between simulation and measurement

As the purpose of FEA was to extract pressure distributions rather than obtaining the absolute value of contact pressure, there was no necessity to compare the simulated pressure values with the measurements in details. Generally, the FEA results showed higher pressure magnitudes than sensor values. This was mainly due to the difference between material parameters assigned to the finite element models and properties of real hand tissues. Specifically, the skin parameter assigned to the hand model is harder than overall hand tissues which contain softer materials like fat. Although simulated results were higher than measurement values, assigning a relatively stiffer material to the hand model could avoid omitting pressure spots which could occur if using low Young's modulus materials. However, the drawback of using a harder material parameter was that several unnecessary pressure spots were generated, e.g. spots 2, 9 and 10. Small pressures were measured as the tissues are considerably softer at these locations, so they were excluded from critical spots.

F. Limitations

Since the study used discrete categorical scales to measure the discomfort rather using continuous analogue, some subjects may present inaccurate ratios at some spots, especially with discomfort scores 0 and 1. For instance, at spot 2, since all subjects reported discomfort scores of 0 and no contact pressure was measured, it had no ratio. However, it does not mean there is no sensitivity at this location. For this study, it was unnecessary to investigate the ratio at spot 2 in terms of wearing the two types of orthoses. Also, if the discomfort score was reported as 1 due to the feeling of a gentle contact, the ratio could be high due to very low contact pressure measured. For example, although spot 5 showed relatively higher ratio than some other spots, only two subjects reported discomfort levels higher than score 1 with scores 2 and 3 at the location. Therefore, though high ratios were shown at some spots, the objective and subjective measurements should be taken into consideration to inform the sensitivity, and the high ratio at some spots may not be harmful and could be negligible, e.g. spots 1, 5, 6, 11 and 12.

Although orthoses were customized by several senior clinicians, as they were from the same clinic, they may apply similar techniques to fabricate orthoses [7]. Thus, the identified critical spots cannot represent hand orthoses fabricated in other clinics. More or fewer pressure spots may be identified using data from different hospitals. However, pressure limits at the critical spots should be similar for patients with the same conditions. Also, the small sample size may limit the accuracy of the ANN. For instance, as no subject reported discomfort score 4 or 5 at the spot 4, the prediction at the two scores may present relatively high errors at this location. In our future study, larger sample size of patients' data in long term wearing will be collected from multiple centers to validate the findings and improve the accuracy of ANN with more training data.

Moreover, this study focused on patients with bone fractures and the measurement was completed on still hands, as the affected hand was immobilized as still as possible according to the clinicians' advice to prevent motions that would aggravate the fracture. However, for patients with other conditions which are not affected by movements, dynamic force may be generated under orthoses. For example, contact pressure under spinal orthosis for scoliosis patients may vary when conducting functional tasks. Dynamic force may also be generated due to specific symptoms, such as clonus and spasticity of stroke patients. Thus, investigating the dynamic force would

be a different study with different subjects. Establishing the relationship between the discomfort and static contact pressure is an essential step enabling further research that expands the proposed method for different conditions with various orthoses to reduce excessive contact pressure during movements.

G. Future application

Soft sensor skins with critical spots can be manufactured, with three sensor units at spots 7, 8 and 13 for WoTS and two additional sensor units at spots 3 and 4 for WTS. In the clinic, the patient's information can be inputted into the established NN to estimate a pressure limit at each critical spot. Using the soft sensor skin attached on the patient's hand during and shortly after orthosis customization, notifications of excessive pressure can be provided for clinicians to adjust the orthosis accurately to mitigate side effects. As a future opportunity, the proposed method can be applied for other static orthoses to mitigate discomfort during the period of immobilization. It also has the potential to be modified with additional dynamic variables and applied for orthoses or prostheses which release symptoms or support functional tasks.

V. Conclusion

This paper for the first time provides a data-driven method to obtain a set of pressure limits to minimize discomfort at critical spots under the two types of hand orthoses (WoTS and WTS). The contact pressure under orthoses for 40 patients were measured using a new soft sensor skin for identification of five critical spots, where the fabrication of orthoses needs special attention to reduce excessive contact pressure that may be commonly developed at these locations. Three critical spots at the abductor digiti minimi, the distal end of ulna and near the anatomic snuffbox were identified under the orthosis type WoTS and two additional spots at the palm side of thumb proximal phalanx and the thumb metacarpophalangeal joint for the orthosis type WTS. For all subjects, the highest average contact pressure was found at the distal end of ulna (0.036 MPa), and an area at the palm side of thumb proximal phalanx showed the highest sensitivity of perception to pressure. The variance of pressure was found at the same discomfort level due to different perception of individuals. The general pressure limits at the five critical spots were predicted using ANN with satisfactory accuracy (R^2 of testing set as 0.9, 0.97, 0.88, 0.81 and 0.89 respectively). Different pressure limits were also revealed between the two types of orthoses at the two critical spots on wrist due to different sensitivity related to conditions. The prediction of a pressure limit for individual patient enables clinicians to adjust orthosis at the key area without subjective feedback from patients. The adjustment can be conducted depending on the sensor reading which should be a bit lower than the predicted pressure due to the prediction error (MAE). This method has the potential to improve patients' experience by reducing the variability of manual orthosis adjustments. It also provides a platform for researchers to further investigate the pressure in the non-static situation for patents with other conditions such as scoliosis or stroke, and has implications for training of clinicians.

References

[1] E. E. Fess and C. A. Philips, *Hand splinting: principles and methods*. Mosby Incorporated, 1987.

[2] T. Richards, R. Clement, I. Russell, and D. Newington, "Acute hand injury splinting–the good, the bad and the ugly," *Ann. R. Coll. Surg. Engl.*, vol. 100, no. 2, pp. 92–96, 2018.

[3] J. Buurke, J. Grady, J. De Vries, and C. T. Baten, "Usability of thenar eminence orthoses: report of a comparative study," *Clinical rehabilitation*, vol. 13, no. 4, pp. 288–294, 1999.

[4] D. Angelis *et al.*, "Efficacy of a soft hand brace and a wrist splint for carpal tunnel syndrome: a randomized controlled study," *Acta neurologica scandinavica*, vol. 119, no. 1, pp. 68–74, 2009.

[5] J. M. Bednar, "The treatment of hand fractures by the application of casts and splints," *Oper. Tech. Orthop.*, vol. 7, no. 2, pp. 93–95, 1997.

[6] D. R. Berlowitz and D. M. Brienza, "Are all pressure ulcers the result of deep tissue injury? a review of the literature," *Ostomy Wound Management*, vol. 53, no. 10, p. 34, 2007.

[7] X. Tan, W. Chen, J. Cao, and S. Ahmed-Kristensen, "A preliminary study to identify data needs for improving fit of hand and wrist orthosis using verbal protocol analysis," *Ergonomics*, pp. 1–14, 2020.

[8] I. Hoogendoorn, J. Reenalda, B. F. Koopman, and J. S. Rietman, "The effect of pressure and shear on tissue viability of human skin in relation to the development of pressure ulcers: a systematic review," *Journal of tissue viability*, vol. 26, no. 3, pp. 157–171, 2017.

[9] S. Mansfield *et al.*, "Pressure injury prevention: A survey," *IEEE reviews in biomedical engineering*, vol. 13, pp. 352–368, 2019.

[10] Y. Akiyama, S. Okamoto, Y. Yamada, and K. Ishiguro, "Measurement of contact behavior including slippage of cuff when using wearable physical assistant robot," *IEEE Transactions on Neural Systems and Rehabilitation Engineering*, vol. 24, no. 7, pp. 784–793, 2015.

[11] M. Hopkins, R. Vaidyanathan, and A. H. McGregor, "Examination of the performance characteristics of velostat as an in-socket pressure sensor," *IEEE Sensors Journal*, 2020.

[12] Z. O. Abu-Faraj, G. F. Harris, and P. A. Smith, "Surgical rehabilitation of the planovalgus foot in cerebral palsy," *IEEE Transactions on neural systems and rehabilitation engineering*, vol. 9, no. 2, pp. 202–214, 2001.

[13] N. Hegde *et al.*, "The pediatric smartshoe: wearable sensor system for ambulatory monitoring of physical activity and gait," *IEEE transactions on neural systems and rehabilitation engineering*, vol. 26, no. 2, pp. 477–486, 2017.

[14] Y. Cha, "Changes in the pressure distribution by wrist angle and hand position in a wrist splint," *Hand Surgery and Rehabilitation*, vol. 37, no. 1, pp. 38–42, 2018.

[15] E. Chalmers, E. Lou, D. Hill, V. H. Zhao, and M.-S. Wong, "Development of a pressure control system for brace treatment of scoliosis," *IEEE Transactions on Neural Systems and Rehabilitation Engineering*, vol. 20, no. 4, pp. 557–563, 2012.

[16] X. Tan, L. He, J. Cao, W. Chen, and T. Nanayakkara, "A soft pressure sensor skin for hand and wrist orthoses," *IEEE Robotics and Automation Letters*, vol. 5, no. 2, pp. 2192–2199, 2020.

[17] M. B. Yandell *et al.*, "Characterizing the comfort limits of forces applied to the shoulders, thigh and shank to inform exosuit design," *Plos one*, vol. 15, no. 2, p. e0228536, 2020.

[18] K. Hokari *et al.*, "The relationships of gripping comfort to contact pressure and hand posture during gripping," *International Journal of Industrial Ergonomics*, vol. 70, pp. 84–91, 2019.

[19] Y.-K. Kong *et al.*, "Comparison of comfort, discomfort, and continuum ratings of force levels and hand regions during gripping exertions," *Applied Ergonomics*, vol. 43, no. 2, pp. 283–289, 2012.

[20] M. Kolich, "Predicting automobile seat comfort using a neural network," *Int. J. Ind. Ergon.*, vol. 33, no. 4, pp. 285–293, 2004.

[21] S. Lu, J. Su, Q. Xiang, J. Zhou, and M. Wu, "Accuracy of self-reported height, weight, and waist circumference in a general adult chinese population," *Population health metrics*, vol. 14, no. 1, p. 30, 2016.

[22] S. Lloyd, "Least squares quantization in pcm," *IEEE transactions on information theory*, vol. 28, no. 2, pp. 129–137, 1982.

[23] C. E. Osgood, G. J. Suci, and P. H. Tannenbaum, *The measurement of meaning*. University of Illinois press, 1957, no. 47.

[24] U. Zafar *et al.*, "Correlation between height and hand size, and predicting height on the basis of age, gender and hand size," *Journal Of Medical Sciences*, vol. 25, no. 4, pp. 425–428, 2017.

[25] P. J. Keir *et al.*, "Guidelines for wrist posture based on carpal tunnel pressure thresholds," *Human factors*, vol. 49, no. 1, pp. 88–99, 2007.

[26] B. Stark, T. Carlstedt, R. Hallin, and M. Risling, "Distribution of human pacinian corpuscles in the hand: a cadaver study," *The Journal of Hand Surgery: British & European Volume*, vol. 23, no. 3, pp. 370–372, 1998.